Targeting AKT/mTOR and ERK MAPK signaling inhibits hormone-refractory prostate cancer in a preclinical mouse model

Carolyn Waugh Kinkade,[1] Mireia Castillo-Martin,[2,3] Anna Puzio-Kuter,[1,3] Jun Yan,[1,3] Thomas H. Foster,[4] Hui Gao,[5] Yvonne Sun,[5] Xuesong Ouyang,[5] William L. Gerald,[6,7] Carlos Cordon-Cardo,[1,2,3] and Cory Abate-Shen[1,2,3,5]

[1]Department of Urology, [2]Department of Pathology, and [3]Herbert Irving Comprehensive Cancer Center, Columbia University College of Physicians and Surgeons, New York, New York, USA. [4]Urologic University Clinic of Basel, Basel, Switzerland. [5]Center for Advanced Biotechnology and Medicine and The Cancer Institute of New Jersey, Robert Wood Johnson Medical School, University of Medicine & Dentistry of New Jersey, Piscataway, New Jersey, USA. [6]Department of Pathology and [7]Department of Human Oncology and Pathogenesis, Memorial Sloan-Kettering Cancer Center, New York, New York, USA.

The AKT/mammalian target of rapamycin (AKT/mTOR) and ERK MAPK signaling pathways have been shown to cooperate in prostate cancer progression and the transition to androgen-independent disease. We have now tested the effects of combinatorial inhibition of these pathways on prostate tumorigenicity by performing preclinical studies using a genetically engineered mouse model of prostate cancer. We report here that combination therapy using rapamycin, an inhibitor of mTOR, and PD0325901, an inhibitor of MAPK kinase 1 (MEK; the kinase directly upstream of ERK), inhibited cell growth in cultured prostate cancer cell lines and tumor growth particularly for androgen-independent prostate tumors in the mouse model. We further showed that such inhibition leads to inhibition of proliferation and upregulated expression of the apoptotic regulator Bcl-2–interacting mediator of cell death (Bim). Furthermore, analyses of human prostate cancer tissue microarrays demonstrated that AKT/mTOR and ERK MAPK signaling pathways are often coordinately deregulated during prostate cancer progression in humans. We therefore propose that combination therapy targeting AKT/mTOR and ERK MAPK signaling pathways may be an effective treatment for patients with advanced prostate cancer, in particular those with hormone-refractory disease.

Introduction

Prostate cancer is one of the most common neoplasms, particularly among aging males in the United States. Like many adenocarcinomas, prostate tumors arise from preinvasive lesions, mainly prostatic intraepithelial neoplasia (PIN), which ultimately progress to adenocarcinoma and, in some cases, metastatic disease (1). Cancer progression, as well as all aspects of normal prostate differentiation, are critically dependent upon androgen receptor (AR) signaling (2).

While the prognosis for men diagnosed with early-stage disease has improved considerably in recent years, due to advances in the treatment of organ-confined prostate cancer, there are still few effective therapeutic options for advanced prostate cancer (3–5). The most common, namely abrogation of AR signaling via hormone deprivation therapy, is initially effective but ultimately leads to a hormone-refractory form of the disease, which is usually highly aggressive and frequently lethal. Although advances in chemotherapy have improved patient outcome (4–7), there remains a clear need for effective mechanism-based therapeutic approaches that can achieve long-term improvements in patient outcome.

Among the major signaling networks that have been implicated in advanced prostate cancer are the AKT/mammalian target of rapamycin (AKT/mTOR) and MAPK pathways. Indeed, deregulated expression and/or mutations of the phosphate and tensin homolog tumor suppressor gene (*PTEN*) occur with high frequency in prostate cancer, leading to aberrant activation of AKT kinase activity as well as its downstream effectors, including the mTOR signaling pathway (e.g., refs. 8–11). In addition, many prostate tumors display deregulated growth factor signaling, which may result in activation of MAPK kinase 1 (MEK) kinase and ultimately ERK MAP signaling (e.g., refs. 12, 13). Notably, previous studies have demonstrated that the AKT/mTOR and MAPK signaling pathways are alternatively and/or coordinately expressed in advanced prostate cancer and function cooperatively to promote tumor growth and the emergence of hormone-refractory disease (8, 11, 13–16). These observations formed the basis for our hypothesis that targeting these signaling pathways combinatorially may be effective for inhibiting tumorigenicity and androgen independence in prostate cancer.

In the current study, we have investigated the consequences of combinatorial inhibition of the AKT/mTOR and ERK MAPK signaling pathways by integrating preclinical studies in a genetically engineered mouse model, with analyses of the status of these pathways in human clinical specimens. We have employed the *Nkx3.1; Pten* mutant mouse model, which recapitulates many features of human prostate cancer (15, 17, 18). In particular, these mutant mice develop PIN, which progresses to adenocarcinoma with high penetrance (>90%) and with a highly reproducible time course of disease progression, while androgen deprivation leads to the emergence of hormone-refractory tumors (Figure 1A) (15, 17, 18). Furthermore, many key molecular pathways that are known to be altered in

Nonstandard abbreviations used: BPH, benign prostatic hyperplasia; CI, combination index; MEK, MAPK kinase 1; mTOR, mammalian target of rapamycin; S6K, p70 S6 kinase; PCa, prostate adenocarcinoma; PIN, prostatic intraepithelial neoplasia; TMA, tissue microarray.

Conflict of interest: The authors have declared that no conflict of interest exists.

Citation for this article: *J. Clin. Invest.* **118**:3051–3064 (2008). doi:10.1172/JCI34764.

human prostate cancer are also altered during cancer progression in these mice (19–21). Most relevant for the current study, *Nkx3.1; Pten* mutant mice display activation of AKT/mTOR and ERK MAPK signaling during prostate cancer progression in androgen-dependent and androgen-independent contexts (15). Therefore, we reasoned that these *Nkx3.1; Pten* mice should provide an excellent preclinical model to test the consequences of combinatorial targeting of AKT/mTOR and ERK MAPK signaling for prostate tumorigenesis.

We now report that combinatorial inhibition of the AKT/mTOR and ERK MAPK signaling pathways is highly effective for inhibition of prostate tumorigenicity in vivo, particularly for androgen-independent tumors. Furthermore, our analyses of the status of the PTEN/AKT/mTOR signaling pathway in human prostate tumors, as well as its correlation with activation of ERK MAPK signaling, confirm that these pathways are frequently deregulated in human prostate cancer and are, therefore, suitable targets for therapeutic intervention. We propose that combination therapy targeting the AKT/mTOR and ERK MAPK signaling pathways may be applicable to a broad spectrum of patients with advanced prostate cancer, particularly those with hormone-refractory disease, for which novel treatment options are urgently needed.

Results

Inhibition of AKT/mTOR and ERK MAPK signaling pathways with rapamycin and PD0325901. Based on previous studies showing that AKT/mTOR and ERK MAPK signaling pathways synergize to promote prostate tumorigenicity in human prostate cancer cell lines in culture as well as in *Nkx3.1; Pten* mutant mice in vivo (15, 16), we hypothesized that targeted therapy to combinatorially inhibit these signaling pathways would be effective for blocking prostate tumor growth. Therefore, we developed experimental paradigms to test the consequences of inhibiting these pathways individually or together in androgen-dependent and androgen-independent prostate tumors in the *Nkx3.1; Pten* mutant mice (Figure 1A).

In deciding upon the appropriate agents to test this hypothesis, our primary considerations were: (a) the accessibility/availability of relevant small-molecule inhibitors for these pathways; (b) the appropriateness of such agents for use in vivo as well as in cell culture; and (c) the feasibility of using such agents combinatorially. To achieve inhibition of ERK MAPK signaling, we opted to target MEK kinase, since it is directly upstream of ERK, which is considered to be its primary target (12). Notably, several MEK inhibitors are now available that have been shown to have potent anticancer growth properties, some of which are currently in clinical trials (22–24). For these studies, we used PD0325901 (from Pfizer), which is similar to its predecessor CI-1040 (24), albeit reported to have improved potency (22).

In lieu of AKT, effective inhibitors for which are still not widely available, we chose to target mTOR, since many of the downstream consequences of the AKT kinase are thought to be mediated through mTOR signaling (25, 26) and since components of the mTOR pathway have been shown to be activated in advanced prostate cancer (10). Moreover, unlike inhibitors of AKT, inhibitors of mTOR, namely rapamycin and its derivatives (e.g., CCI-779 from Wyeth and RAD001 from Novartis), are now readily available and considered to be promising anticancer agents (27). Notably, although their efficacy as single agents may be limited, rapamycin and related compounds are considered to be particularly suitable for use in combination therapy (e.g., refs. 27, 28). For these preclinical studies, we chose to use rapamycin (rather than one of the newer derivatives), since it is commercially available and therefore logistically more feasible to use in combination with PD0325901, which is obtained from Pfizer.

Although rapamycin and PD0325901 have been used as single agents in genetically engineered mice (24, 29–33), it was first necessary to define the optimal experimental parameters for their use in combination in vivo. To do so, we performed pilot studies in the *Nkx3.1; Pten* mutant mice to verify the optimal dosage as well as the appropriate dosing schedule for the agents delivered individually or in combination. For these and most subsequent studies, we used phosphorylation of S6 (p-S6), which is downstream of mTOR, as an indicator of mTOR pathway activity and phosphorylation (i.e., activation) of ERK MAPK as an indicator of MEK inhibition.

In general, we found that the optimal use of these agents in combination was similar to their previously reported use as single agents. In particular, we found that a single dose of rapamycin plus PD0325901 delivered to the *Nkx3.1; Pten* mutant mice individually or together resulted in the effective inhibition of their respective targets (i.e., p-S6 and p-ERK, respectively) for up to 24 hours (Figure 1B). Moreover, we found that the appropriate doses of rapamycin and PD0325901 needed to achieve effective inhibition of their respective targets, while resulting in limited toxicity or loss of body weight (see Supplemental Table 1; supplemental material available online with this article; doi:10.1172/JCI34764DS1), were similar to those in published reports for their use as single agents. In particular, we found that i.p. delivery of 10 mg/kg of rapamycin resulted in significant inhibition of p-S6, and conversely that oral delivery of 20 mg/kg of PD0325901 resulted in effective inhibition of p-ERK, as evident by immunostaining and Western blot analyses of prostate tissues (Figure 1, B–J). Therefore, for these preclinical studies, we implemented a once-daily dosing schedule using 10 mg/kg of rapamycin and/or 20 mg/kg of PD0325901.

Rapamycin and PD0325901 synergize to inhibit prostate cell growth in culture. To quantify the individual and combinatorial effects of rapamycin and PD0325901, we performed studies in culture using mouse CASP prostate cancer cell lines, which were generated from primary tumors from the *Nkx3.1; Pten* mutant mice and include both androgen-responsive (CASP 2.1) and androgen-independent (CASP 1.1) lines (15, 19). First, we evaluated the IC_{50} of the single agents, which was 0.3 nM for rapamycin and 40 nM for PD0325901 in these CASP cells (Figure 2, A and B). In contrast, the IC_{50} of the agents in combination was shifted to 0.0018 nM for rapamycin and 11 nM for PD0325901 (Figure 2, C and D). To determine whether the shift in IC_{50} for the combination reflected their synergism in cell culture, we assessed their combination index (CI), which, as calculated based on the Chou-Talalay equation, provides a means of quantifying the differential sensitivity of agents in combination (34). The CI takes into account both potency (IC_{50}) and the shape of the dose-effect curve, such that a CI value of less than 1 indicates synergism, a CI value of 1 indicates an additive effect, while a value greater than 1 indicates antagonism. We found that rapamycin and PD0325901 displayed extremely low CIs (i.e., in the range of 0.03–0.1; Figure 2E), indicating their strong synergism in cell culture.

To gain initial insights regarding the mechanistic basis for the combinatorial effects of rapamycin and PD0325901, we investigated the expression status of various apoptotic regulatory proteins. We found that Bim (35, 36) was upregulated in response to the drug treatment, which is notable, since it has been shown to be upregulated by inhibitors of mTOR and MEK in other cell types

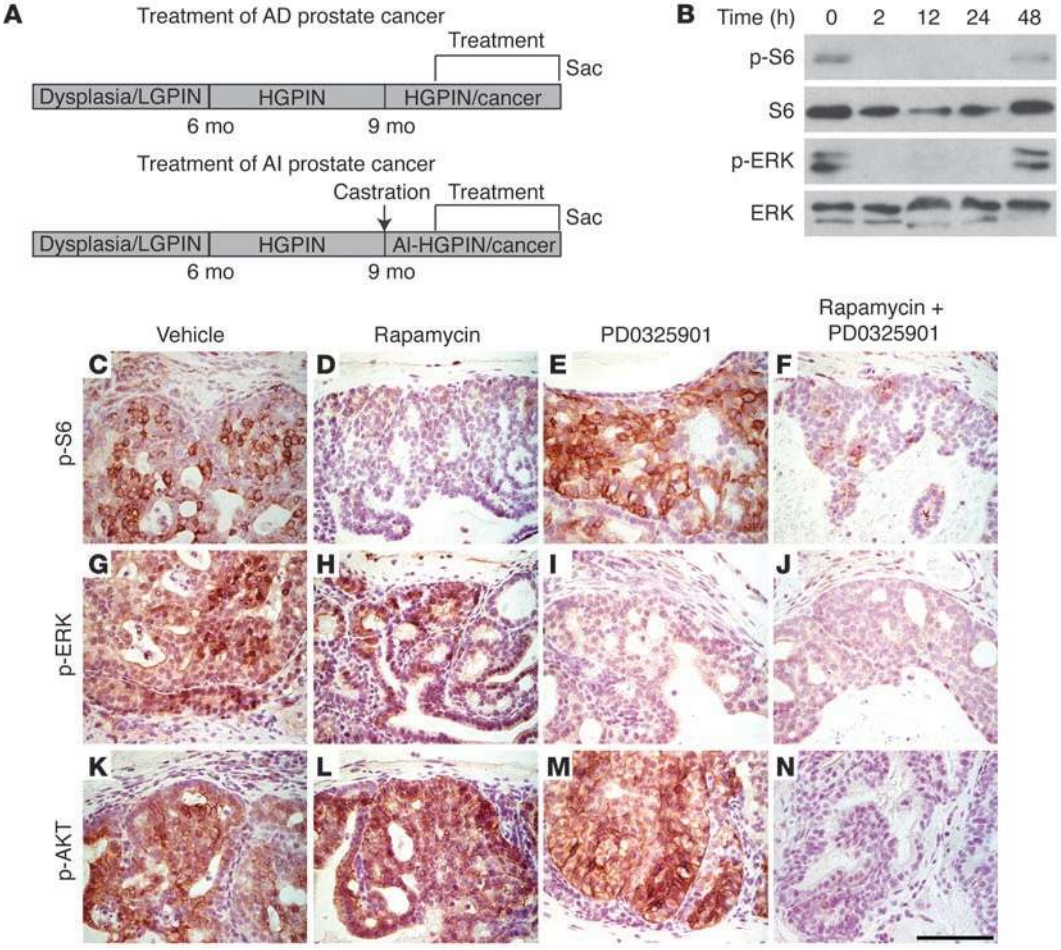

Figure 1

Inhibition of AKT/mTOR and ERK MAPK signaling pathways with rapamycin and PD0325901. (**A**) Diagram of the experimental strategy. *Nkx3.1; Pten* mutant mice develop low-grade and high-grade PIN (LGPIN and HGPIN, respectively) and ultimately adenocarcinoma as a consequence of aging, as well as androgen independence following castration. The trial design entailed enrolling androgen-intact or androgen-ablated mutant (or control) mice at approximately 10 months of age randomly into groups that were treated with rapamycin and/or PD0325901 (or vehicle) for 21 days (5 days on/2 days off), after which the mice were sacrificed (Sac) for analyses of end points (i.e., histology, prostate weights, cellular proliferation, immunohistochemistry, and Western blot analyses; Figures 3–6 and Table 1). AD, androgen-dependent; AI, androgen-independent. (**B**) Rapamycin and PD0325901 inhibit their respective targets in the prostate for up to 24 hours. Western blot analyses were performed using protein extracts prepared from the dorsolateral prostate of *Nkx3.1*$^{+/-}$*Pten*$^{+/-}$ mutant mice (10 months) treated with rapamycin plus PD0325901 for the times indicated. Each group had 3 mice; Western blot analyses were done with at least 2 independent mice in each group, and representative samples are shown. (**C**–**N**) Rapamycin and PD0325901 lead to inhibition of target proteins in mouse prostate tissues in vivo. Immunohistochemical analyses were performed using the indicated antibodies on sections from the anterior prostate of *Nkx3.1*$^{+/-}$*Pten*$^{+/-}$ mutant mice (10 months; androgen-intact) treated with rapamycin and/or PD0325901 (or vehicle) as indicated for 1 week. Scale bar: 100 μm.

(e.g., ref. 37). Notably, while rapamycin and PD0325901 effectively inhibited their target pathways when used individually or in combination, upregulation of Bim expression was most marked when the drugs were used in combination (Figure 2F). Furthermore, we found that siRNAi-mediated knockdown of Bim resulted in a partial rescue of the consequences for cell survival in MTT assays, suggesting that the activity of these agents is mediated at least in part by upregulation of Bim (Figure 2G).

Collectively, these data suggest that rapamycin and PD0325901 act synergistically to promote cell death in culture, which reflects, at least in part, their combinatorial effects on the apoptotic regulator Bim. Furthermore, although our study is primarily focused on the efficacy of these agents in mutant mice, we have found that these agents also inhibit their respective pathways in human prostate cancer cells (Supplemental Figure 1), which suggests that these agents may have a similar benefit in human prostate cancer.

Preclinical analyses of combination therapy with rapamycin and PD0325901. Having demonstrated the combinatorial efficacy of rapamycin and PD0325901 for inhibiting their respective target pathways in prostate cells in vivo and in culture, as well as having established optimal experimental conditions for their combined use in vivo, we next investigated their potential antitumor effects in *Nkx3.1; Pten* mutant mice. In particular, we performed preclinical studies to compare the consequences of these agents for: (a) treatment of androgen-dependent prostate cancer (i.e., in mice that were androgen-intact); and (b) treatment of androgen-inde-

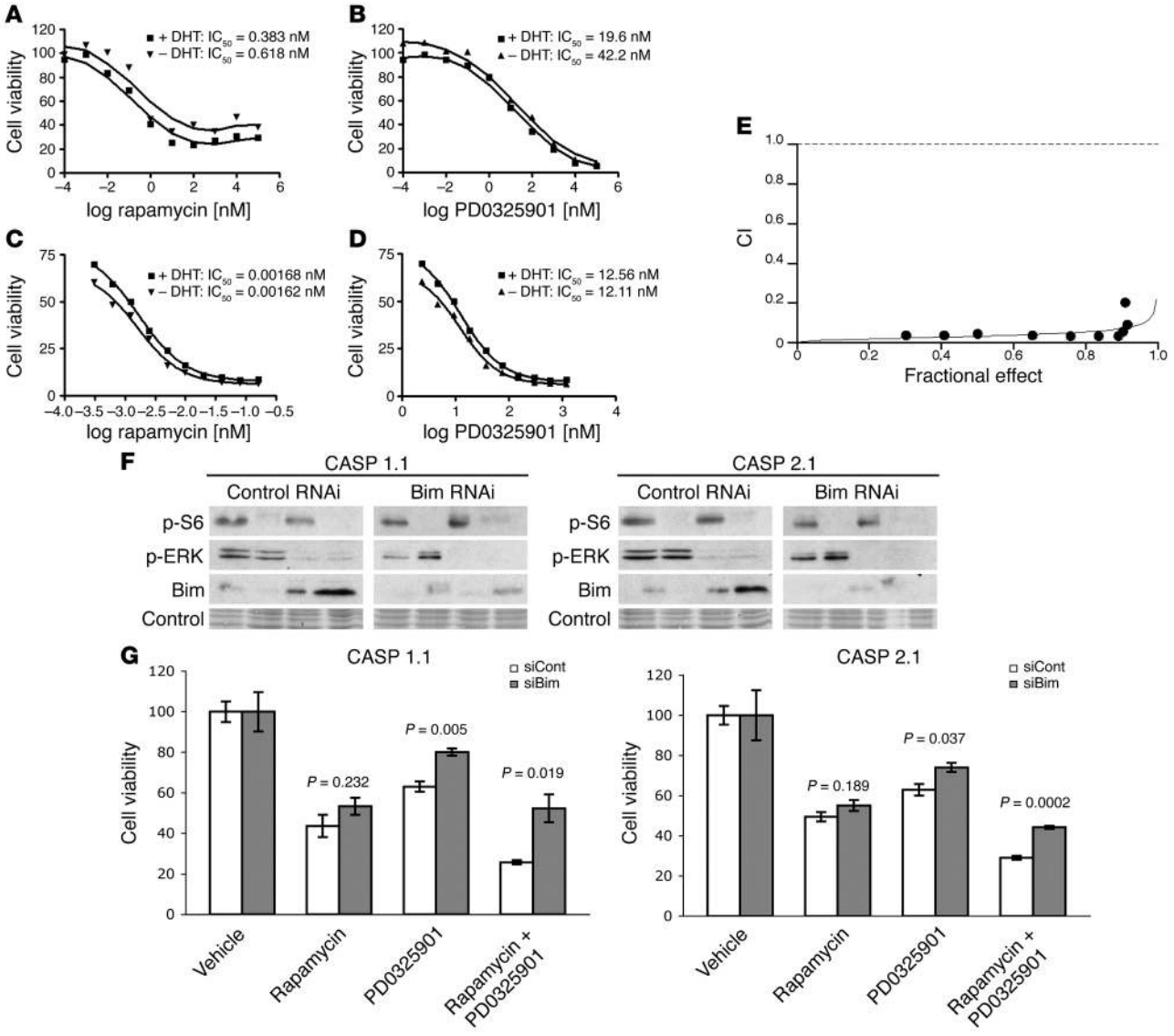

Figure 2

Rapamycin and PD0325901 display strong synergism in cell culture. (**A**–**D**) Analyses of IC_{50} plots for the single agents (**A** and **B**) and the combination agents (**C** and **D**). (**E**) Graphic representation of the CI for rapamycin and PD0325901. These data are shown for CASP 1.1 cells; similar results were obtained for CASP 2.1 cells (not shown). Note that CI values were well below 0.1, indicating strong synergism of the drugs. (**F** and **G**) Bim is upregulated in response to drug treatment. CASP 1.1 or CASP 2.1 cells were transfected with a control or Bim siRNAi, followed by treatment with vehicle or the indicated compounds in the medium for 48 hours. (**F**) Western blot analyses done on whole cell extracts using the indicated antibodies or a control for protein loading (Ponceau S staining). (**G**) Results of MTT assays, indicating the enhanced cell survival in the drug-treated cells following treatment with Bim siRNAi. The *P* values compare the control (siCont) and the Bim siRNAi (siBim) in each group. Data are expressed as mean ± SEM.

pendent prostate cancer (i.e., in mice that had been castrated and had developed hormone-refractory tumors) (Figure 1A).

We used *Nkx3.1; Pten* mutant mice (i.e., *Nkx3.1*$^{+/-}$*Pten*$^{+/-}$ or *Nkx3.1*$^{-/-}$*Pten*$^{+/-}$) or wild-type littermates (i.e., *Nkx3.1*$^{+/+}$*Pten*$^{+/+}$) at 10–12 months, by which age the mutant mice display virtually complete penetrance of high-grade PIN with associated adenocarcinoma, as well as complete penetrance of hormone-refractory tumors following surgical castration (Figure 1A) (15, 17, 18). Cohort groups were composed of mutant (or control) mice randomly assigned to receive vehicle alone, single agents (rapamycin or PD0325901), or the combination therapy (rapamycin plus PD0325901) (Table 1 and Supplemental Table 1). Agents were provided for a period of 3 weeks using a dosage schedule of once daily for 5 days, with 2 days off to allow the mice to recover. Endpoint analyses included semiquantitative histological, immunohistochemical, and Western blot analyses, as well as quantitative assessments of prostate tissue weights and proliferation index (Figures 3–5; summarized in Table 1 and Supplemental Table 1); notably, we assessed outcome based on analyses of the combination of these various endpoints rather than any individual parameter.

To augment these studies in the whole animal, we performed complementary studies using a tissue recombination model in

Table 1
Data summary

Experimental group	No. of mice	Tumor weight		Proliferation	
		Fold change	*P*	Fold change	*P*
Paradigm 1: Treatment of AD cancer					
Vehicle	6	NA	NA	NA	NA
Rapamycin	4	2.25	0.066	2.05	0.175
PD0325901	4	0.88	0.453	1.66	0.197
Rapamycin + PD0325901	5	1.73	0.111	2.44	0.165
Paradigm 2: Treatment of AI cancer					
Vehicle	9	NA	NA	NA	NA
Rapamycin	5	1.38	0.062	2.13	0.032
PD0325901	6	1.30	0.041	2.74	0.008
Rapamycin + PD0325901	10	2.18	0.0002	14.64	0.0001
Paradigm 3: Adjuvant therapy of AI cancer					
Vehicle	6	NA	NA	NA	NA
Rapamycin	8	2.18	0.022	2.56	0.071
PD0325901	8	3.00	0.010	3.21	0.022
Rapamycin + PD0325901	12	3.32	0.012	3.35	0.035

AD, androgen-dependent; AI, androgen-independent.

which prostate epithelium from *Nkx3.1; Pten* mutant (or wild-type) mice is combined with wild-type rat mesenchyme and grown under the kidney capsule of androgen-intact or androgen-ablated *nude* male hosts (15) (Figure 6 and Supplemental Table 1). This strategy complements studies done in the whole animal (i.e., in the *Nkx3.1; Pten* mutant mice) in 2 important respects. First, it enables evaluation of the efficacy of combination therapy in vivo for the intended target cells (i.e., the prostate epithelial cells), as opposed to the target tissue (i.e., intact prostate). Second, because of the nature of how the tissue recombinants are made, tumor growth is relatively uniform (and therefore more easily quantified) in the tissue recombination model, in contrast to the intrinsically more heterogenous tumor growth that occurs in the whole animal. However, since preclinical studies are inherently more meaningful in the context of the whole animal with an intact immune response, studies done in the *Nkx3.1; Pten* mutant mice and the tissue recombination model are complementary, not redundant.

Combination therapy with rapamycin and PD0325901 is potently antitumorigenetic for androgen-independent prostate cancer. To test the efficacy of rapamycin and PD0325901 for the treatment of androgen-dependent prostate cancer, we performed preclinical studies in androgen-intact *Nkx3.1; Pten* mutant mice as well as in tissue recombinants grown in androgen-intact *nude* male hosts using the experimental conditions outlined above (Figure 3, Figure 5, A–D, Figure 6, A–H, Table 1, and Supplemental Table 1). We found that, whether delivered individually or in combination, rapamycin and PD0325901 effectively inhibited their respective target pathways in prostate tissues, as evidenced by immunohistochemistry and Western blot analysis for p-S6 and p-ERK (Figure 3, F–M, and Figure 5D). Notably, in combination, these agents resulted in a more striking inhibition of their target proteins, as well as inhibition of p-AKT (Figure 3, B–Q, and Figure 5D).

Nonetheless, both the single agents and the combination were only modestly effective for inhibiting prostate tumorigenicity in this context. For example, the combination therapy produced a modest, albeit not statistically significant, reduction in prostate weight in the whole animal (1.7-fold; $P = 0.111$) and proliferation rate (2.4-fold; $P = 0.165$) (Figure 3, R–U, Figure 5, B and C, and Table 1). However, in the tissue recombinant model, the drug combination did result in a significant inhibition of tumor size (2.6-fold; $P = 0.033$) (Figure 6, A–H), which likely reflects the uniformity of tumor growth in the tissue recombinants relative to the whole animal. Therefore, although rapamycin and PD0325901 effectively inhibit mTOR and ERK MAPK signaling in androgen-dependent prostate cancer, they do not optimally inhibit tumor growth in this context.

In striking contrast, rapamycin and PD0325901 were highly effective for inhibiting androgen-independent tumor growth in the *Nkx3.1; Pten* mutant mice (Figure 4, Figure 5, E and F, and Figure 6, I–P). In particular, both the single agents and the combination therapy resulted in inhibition of their respective target proteins, p-S6 and p-ERK, although as above, the combination produced a more profound inhibition of these proteins as well as the additional inhibition of p-AKT (Figure 4, B–Q, and Figure 5H). Moreover, while the single agents each resulted in a statistically significant reduction in tumor size and proliferation (see Table 1 and Figure 5, F and G), the combination therapy produced a profound abrogation of the histological phenotype, as well as a significant reduction in tumor weights (2.2-fold; $P = 0.0002$) and cellular proliferation (14.7-fold; $P = 0.0001$) (Figure 4, B–E and R–U, Figure 5, F and G, and Table 1). Moreover, the efficacy of this drug combination for androgen-independent prostate cancer was recapitulated in the tissue recombination model of the disease (3.2-fold; $P = 0.007$) (Figure 6, I–P). These findings demonstrate that combination therapy targeting the AKT/mTOR and ERK MAPK signaling pathways is highly effective for the treatment of hormone-refractory prostate cancer in a preclinical model of the disease.

Considering the profound effects of this combination therapy for inhibiting androgen-independent prostate cancer, we investigated whether this drug combination might also be effective in an adjuvant therapy model for hormone-refractory prostate cancer.

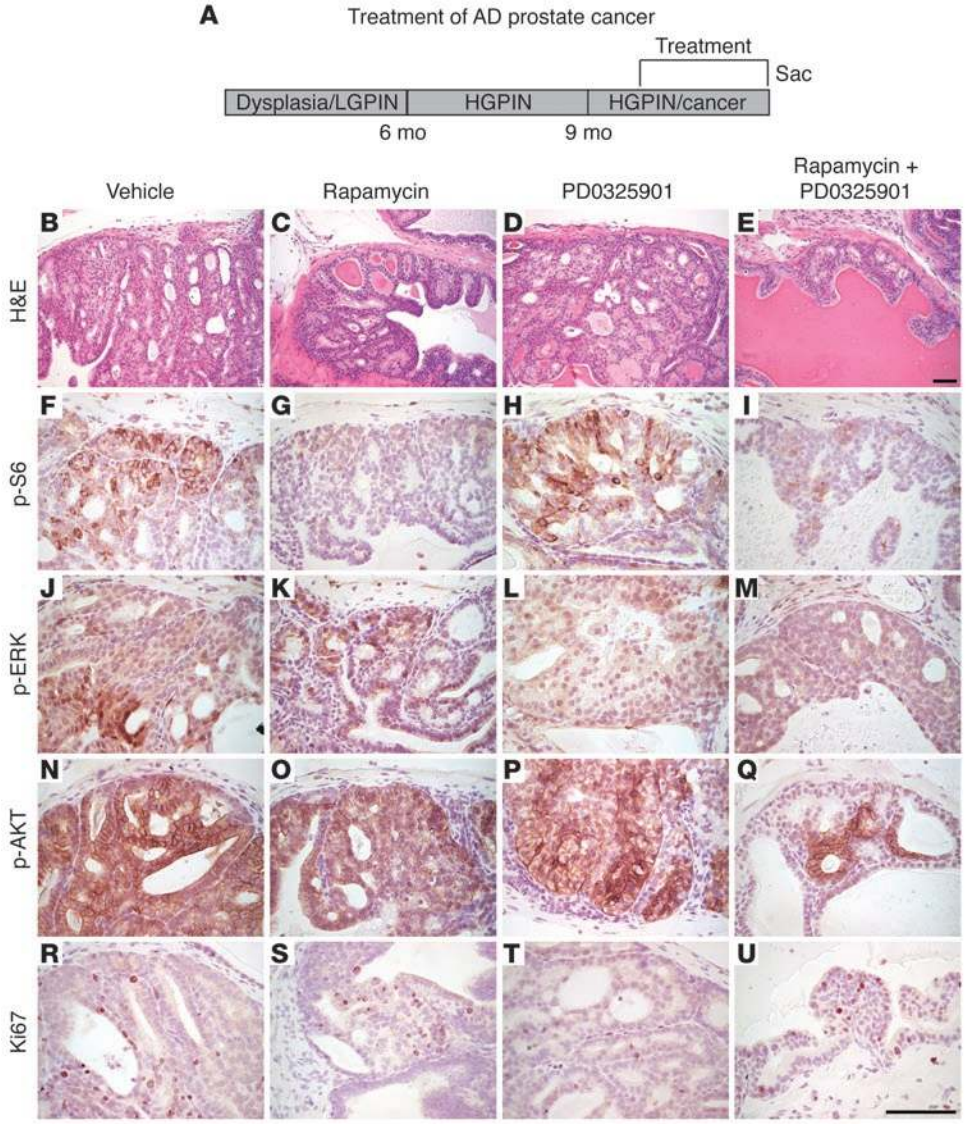

Figure 3
Modest efficacy of rapamycin and PD0325901 for treatment of androgen-dependent prostate cancer. (**A**) Diagram of the experimental strategy, as per Figure 1. (**B**–**U**) Representative tissue sections from the *Nkx3.1*$^{+/-}$*Pten*$^{+/-}$ mutant mice treated with the single agent or combination of agents, showing histological phenotype (H&E) and immunostaining for the antibodies indicated. H&E analyses were performed on all experimental mice in each group; immunohistochemistry was done on a minimum of 4 animals from each group; representative data are shown. Scale bars: 100 μm.

Specifically, rapamycin and PD0325901 were provided for a period of 3 weeks directly following androgen ablation of the *Nkx3.1; Pten* mutant mice or tissue recombinants grown in the *nude* mice (Figure 7 and Table 1). In this context, the drug combination was highly effective for inhibiting prostate tumor growth, as evidenced by the striking effects on the histological phenotype, as well as the significant reduction in the prostate weight (3.3-fold; $P = 0.012$) and cellular proliferation (3.4-fold; $P = 0.035$) in the *Nkx3.1; Pten* mutant mice and in the analogous tissue recombination model (2.2-fold; $P = 0.018$) (Figure 7). Therefore, this combination therapy may be promising for adjuvant therapy of hormone-refractory prostate cancer when used in combination with androgen deprivation therapy.

AKT/mTOR and ERK MAPK signaling pathways are coordinately regulated in human prostate cancer. Extrapolating from these preclinical studies in the mutant mouse model, our findings suggest that combination therapy targeting the AKT/mTOR and ERK MAPK signaling pathways may be beneficial for treatment of patients with hormone-refractory prostate cancer. Notably, the potential to translate these findings from mice to human prostate cancer is particularly promising considering that the combination is effective for inhibiting their target pathways in human prostate cancer cells (Supplemental Figure 1) and since the single agents (or related agents) are already being used in clinical trials (22, 27).

However, the efficacy and expected versatility of the combination therapy depends, in part, upon: (a) the frequency with which these signaling pathways are deregulated individually and combinatorially in human prostate cancer, particularly in patients with advanced disease; and (b) the ease of identifying patients who have primary tumors in which these pathways are deregulated and, therefore, would be appropriate candidates for targeted therapy.

While these issues have been partially addressed in previous studies that have examined the status of individual components of these signaling pathways in human prostate cancer (e.g., refs. 8–11, 13), we have now performed a comprehensive analysis in primary tumors and metastases from human prostate cancer patients to evaluate the coordinate expression of multiple components of the PTEN/AKT/mTOR signaling pathway, as well as their status relative to ERK MAPK signaling (Figure 8 and Table 2). In particular, we performed analyses using 2 independent cohorts of patients assembled on 2 independent tissue microarrays (TMAs). This com-

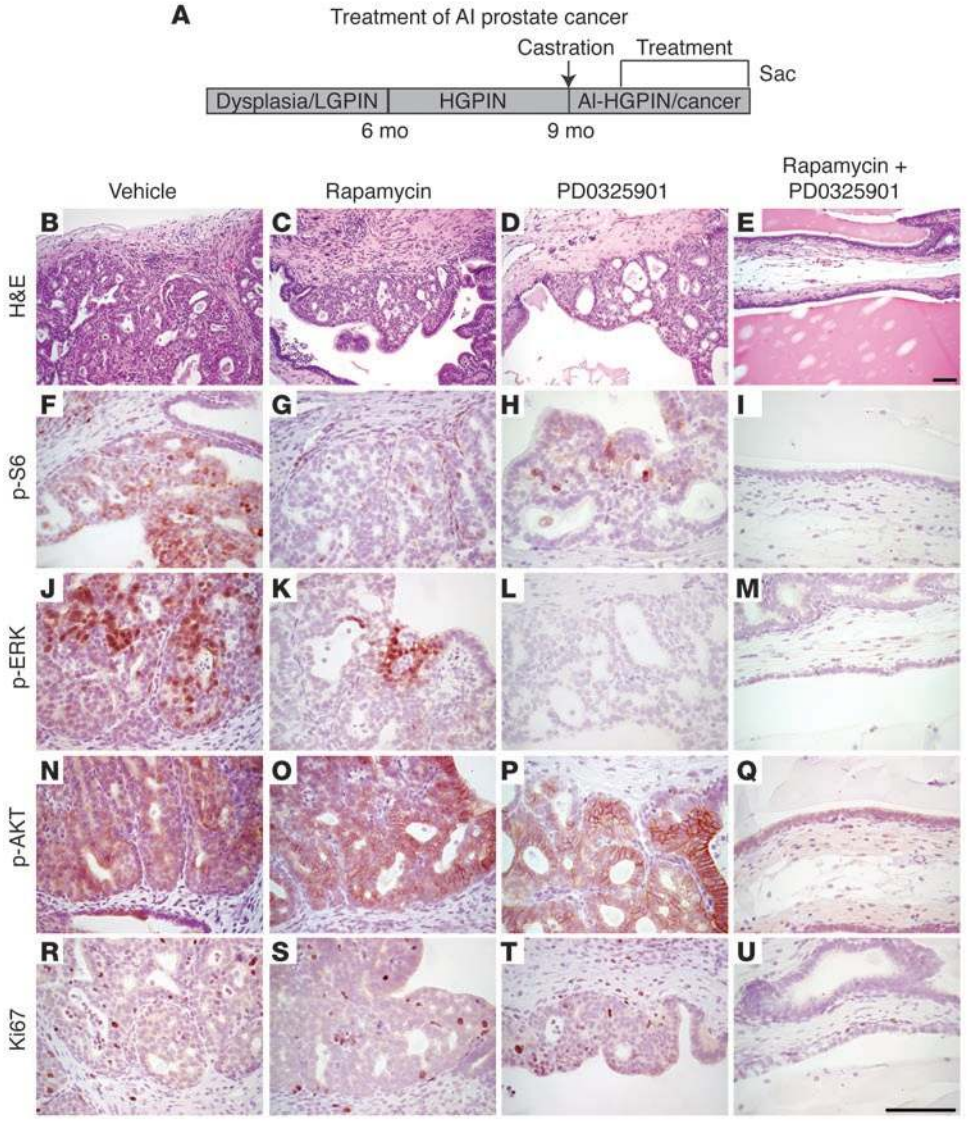

Figure 4
Profound efficacy for prostate histology following treatment of androgen-independent prostate cancer with rapamycin and PD0325901. (**A**) Diagram of the experimental strategy, as per Figure 1. (**B**–**U**) Representative tissue sections from the androgen-ablated *Nkx3.1*$^{+/-}$ *Pten*$^{+/-}$ mutant mice treated with the single or combination of agents, showing histological phenotype (H&E) and immunostaining for the antibodies indicated. In these and all subsequent experiments, H&E analysis was performed on all experimental mice in each group; immunohistochemistry was done on a minimum of 4 animals from each group; representative data are shown. Scale bars: 100 μm.

prehensive series enabled us to examine the coordinate expression of several components of the PTEN/AKT/mTOR pathway, as well as ERK MAPK, in specimens from patients with benign prostatic hyperplasia (BPH); PIN; prostate adenocarcinoma (PCa), including those with low Gleason (≤6) or high Gleason (>7) scores; hormone-refractory cancer; and metastases. In particular, we examined the expression levels of PTEN as well as the activation (phosphorylation) of AKT, mTOR, and p70 S6 kinase (S6K) relative to each other as well as to activation of ERK MAPK.

The first TMA comprised 70 samples, including 25 cases of BPH, 7 of PIN, 19 of low Gleason score cancer, and 19 of high Gleason score cancer (Table 2). We found that PTEN expression was markedly reduced with high frequency (59% cases) during prostate cancer progression, as determined by comparing BPH, PIN, and PCa ($P = 0.05$; Figure 8, A–C; PIN data not shown). We further found that the expression levels of both p-AKT and p-mTOR were significantly elevated in prostate cancer compared with BPH and PIN ($P = 0.001$; Figure 8, D–I; PIN data not shown). Similarly, p-S6K expression was significantly higher in prostate cancer compared with BPH and PIN ($P < 0.0001$; Figure 8, J–L; PIN data not shown). Notably, when activated, these proteins were frequently activated in the same patient samples and also coincident with reduced expression of PTEN (Figure 8, C, F, I, L, and O, and Tables 2–4), indicating that the pathway rather than the individual components are coordinately deregulated.

To further validate these results, as well as the potential clinical implications of identifying an altered PTEN/AKT/mTOR signaling pathway in prostate cancer, we used a second TMA composed of an independent cohort of prostate cancer patients. This TMA represented a large, well-characterized group of 535 patients, including 65 cases of BPH, 78 of PIN, 181 of organ-confined cancer, 120 of hormone-refractory cancer, and 91 of metastatic PCa. We found that decreased levels of PTEN were significantly associated with disease progression, mainly when comparing primary and metastatic prostate cancer ($P = 0.001$). Similarly, increased levels of p-AKT ($P = 0.02$), p-mTOR ($P = 0.02$), and p-S6K ($P = 0.03$) were also found to be significantly associated with tumor progression. Furthermore, these proteins were often activated together and with reduced expression of PTEN, again indicative of deregulation of the signaling pathway.

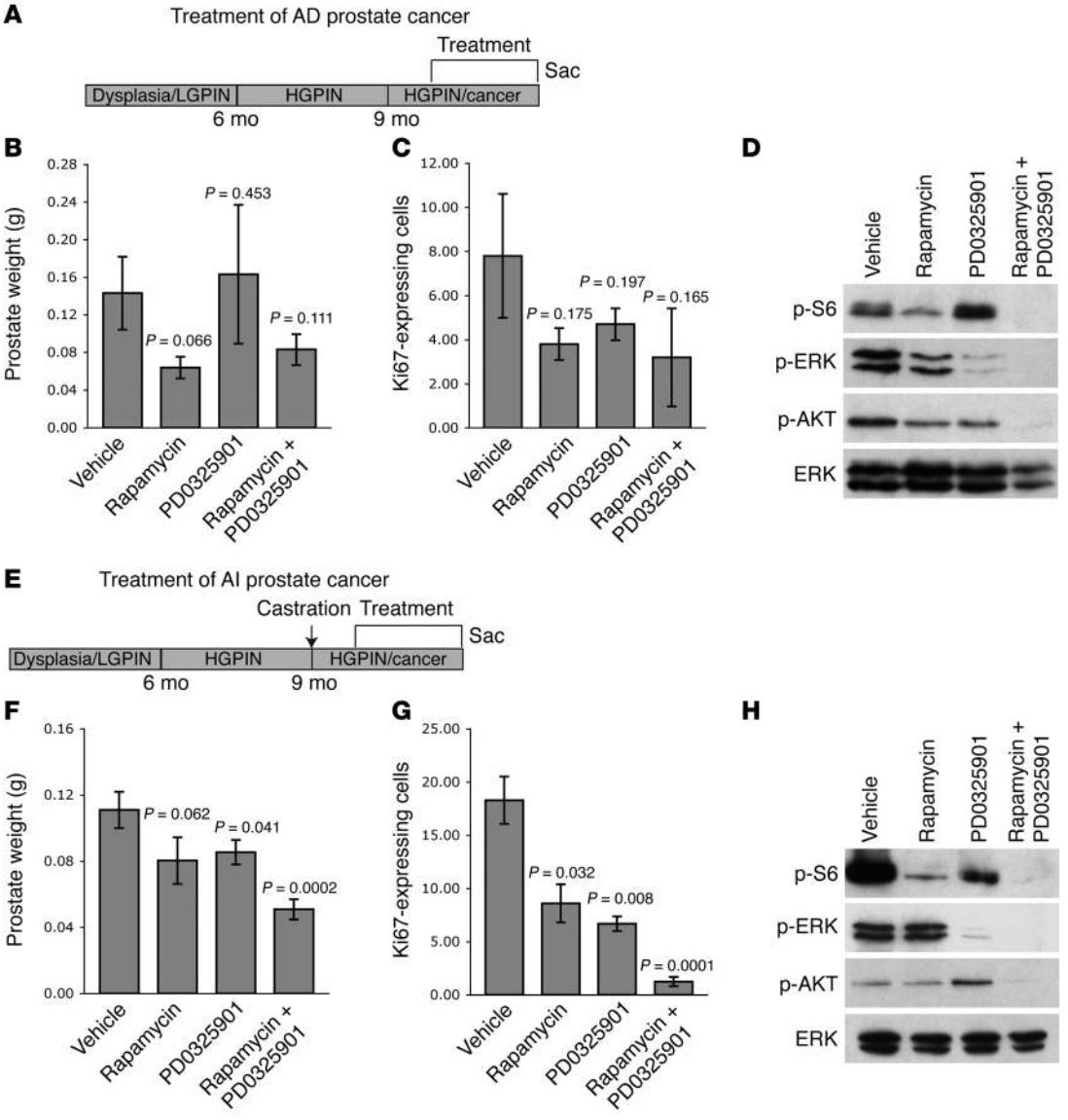

Figure 5

Combination therapy is antitumorigenic for treatment of androgen-independent prostate cancer in *Nkx3.1; Pten* mutant mice. Comparison of the consequences of single agent versus combination therapy for treatment of androgen-dependent (**A**–**D**) or androgen-independent (**E**–**H**) mutant mice. (**A** and **E**) Diagram of the experimental strategy, as per Figure 1. (**B** and **F**) Prostate tissue weights, showing mean ± SEM, with *P* value indicated. (**C** and **G**) Percentage of proliferating cells as determined by Ki67 staining, showing mean ± SEM, with *P* value indicated. (**D** and **H**) Western blots of protein extracts from prostate tissues following treatment. Western blotting was done using a minimum of 3 independent mice in each group; representative data are shown; total ERK is shown as a control for protein loading.

Finally, using this first TMA, we examined the expression of ERK MAPK in human prostate tumor samples, compared with the deregulation of the PTEN/AKT/mTOR signaling pathway (Tables 2–4). Immunohistochemical analysis of p-ERK expression showed that it was focally expressed and at low levels in BPH samples and PIN lesions (Figure 8M; PIN data not shown). However, p-ERK was highly expressed in the majority of cancer samples, and increased levels of ERK MAPK were significantly associated with tumor progression in PIN and low-grade tumors versus high-grade lesions ($P = 0.008$; Figure 8, M–O). Furthermore, when compared with deregulated expression of the PTEN/AKT/mTOR signaling pathway, we found that 21% of patients with prostate cancer displayed deregulated expression of all components of the PTEN/AKT/mTOR signaling pathway as well as ERK MAPK, while 42% of these patients displayed deregulated expression of 1 or more components of the PTEN/AKT/mTOR signaling pathway as well as ERK MAPK (Table 4).

In conclusion, the PTEN/AKT/mTOR signaling pathway is frequently altered in prostate cancer progression and often coincidentally with activation of ERK MAPK signaling. These data support the concept that a substantial number of patients with advanced prostate cancer (conservatively at least 20%) may benefit from combination therapy targeting the AKT/mTOR and ERK MAPK signaling pathways. Furthermore, since the relevant activated target

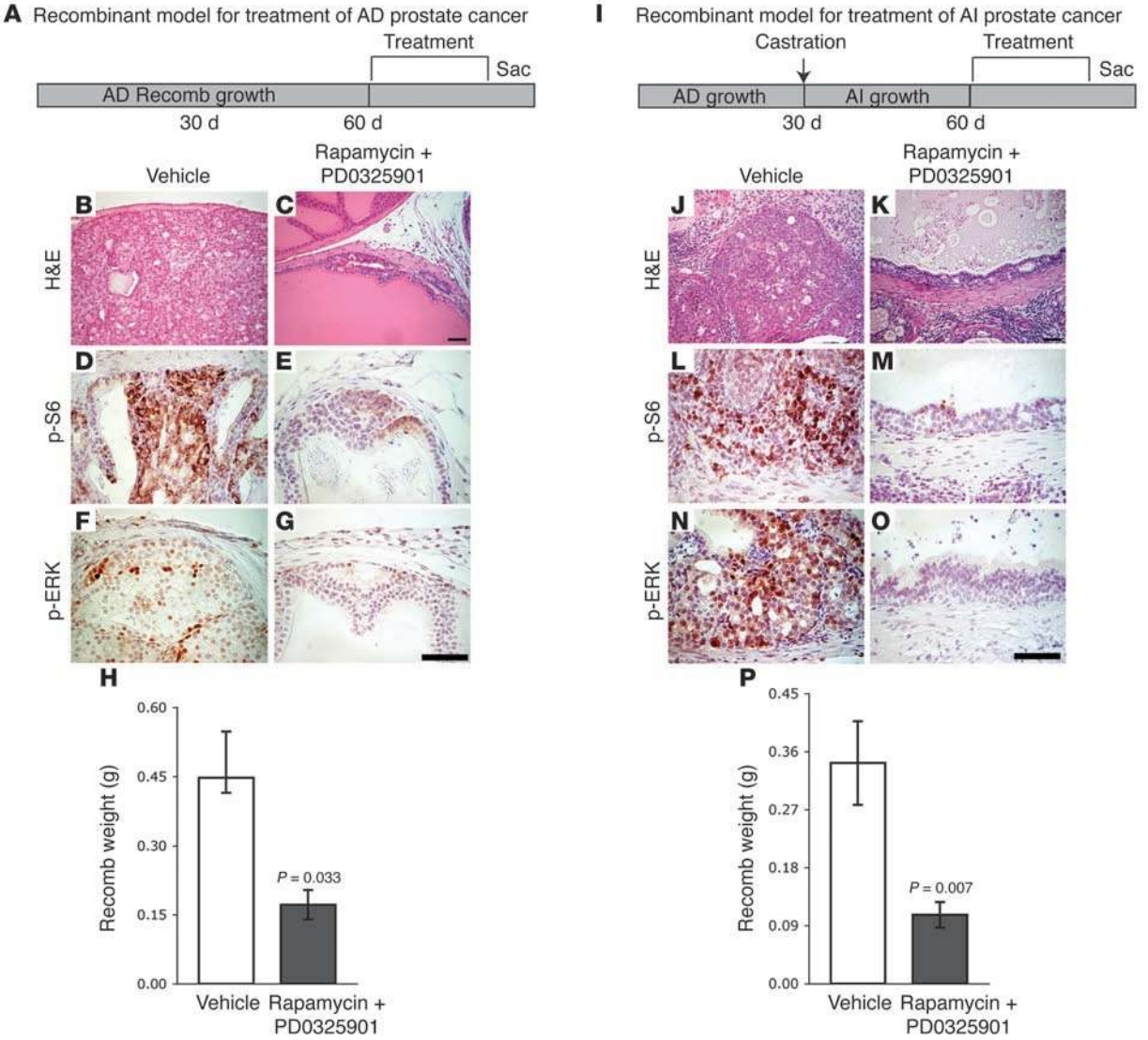

Figure 6

Combination therapy is antitumorigenic in tissue recombination models from the *Nkx3.1; Pten* mutant mice. (**A** and **I**) Diagram of the experimental strategy. Tissue recombinants were made using prostate epithelium from *Nkx3.1; Pten* mutant or wild-type mice and rat embryonic mesenchyme and grown in *nude* mice for 1 month. Following 1 month of growth, the *nude* mice were either left intact (i.e., to model treatment of androgen-dependent prostate cancer) or castrated (i.e., to model treatment of androgen-independent prostate cancer). Mice received rapamycin and/or PD0325901 (or vehicle) for 21 days (5 days on/2 days off), following which the mice were sacrificed for analyses of end points (i.e., histology, prostate weights, and immunohistochemistry). (**B**–**G** and **J**–**O**) Representative tissue sections from the tissue recombinants made from the *Nkx3.1*$^{+/-}$*Pten*$^{+/-}$ prostate epithelium showing histological phenotype (H&E) and immunostaining for p-S6 and p-ERK, as indicated. Scale bars: 100 μm. (**H** and **P**) Weights of the tissue graphs, showing mean ± SEM, with *P* value indicated. Recomb, recombinant.

proteins can be readily detected in primary tumors from patient samples, it should be feasible to identify patients that are most likely to respond to treatment, namely those that display deregulation of PTEN/AKT/mTOR and/or ERK MAPK signaling.

Discussion

In our previous investigations of the molecular mechanisms underlying prostate cancer progression, we found that the AKT/mTOR and ERK MAPK signaling pathways function cooperatively to promote prostate tumorigenicity and androgen independence (15). Based on these findings, we had hypothesized that combinatorial inhibition of these pathways might be effective for the treatment of prostate cancer. We now demonstrate that inhibition of these signaling pathways acts combinatorially to suppress pathway activation and inhibit tumor growth and cellular proliferation in androgen-independent prostate cancer in *Nkx3.1; Pten* mutant mice. Furthermore, analyses of human prostate tumor specimens support the idea that AKT/mTOR and ERK MAPK signaling pathways are frequently activated in prostate tumors, readily detected in advanced human prostate cancer, and are suitable targets for intervention in patients with the disease. We propose that combination therapy targeting the AKT/mTOR and the ERK MAPK signaling pathways may be effective for treatment of a broad spectrum of patients with advanced prostate cancer, particularly those with hormone-refractory disease.

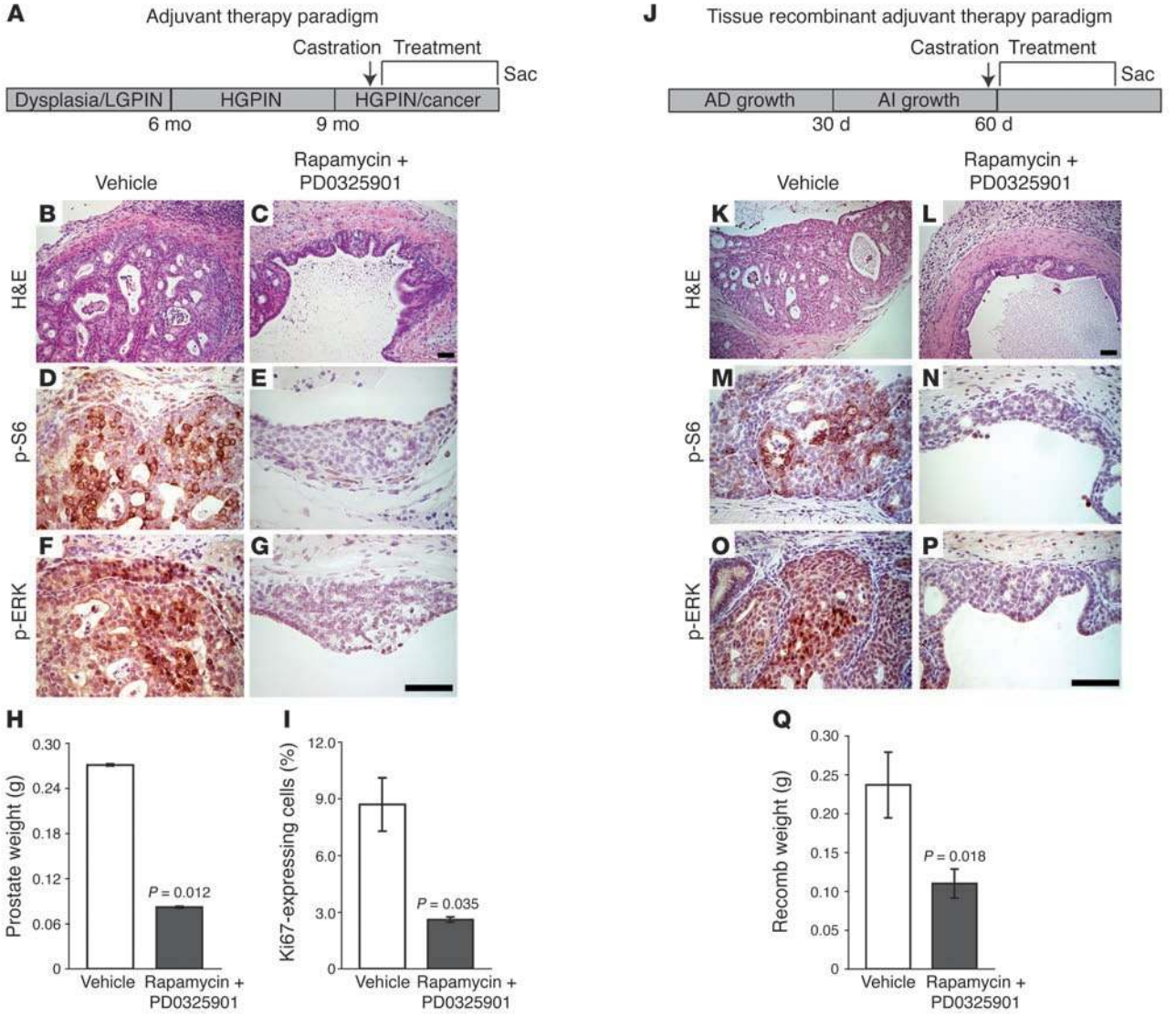

Figure 7

Combination therapy is antitumorigenic in adjuvant therapy of hormone-refractory prostate cancer. (**A**–**I**) Studies in the whole animal. (**A**) Diagram of the experimental strategy. Strategy is similar to that in Figure 1; however, unlike the androgen-independent treatment group, *Nkx3.1*$^{+/-}$ *Pten*$^{+/-}$ mutant mice were castrated immediately prior to receiving the rapamycin and/or PD0325901 (or vehicle) treatment. (**B**–**G**) Representative tissue sections from the *Nkx3.1*$^{+/-}$*Pten*$^{+/-}$ mutant mice showing histological phenotype (H&E) and immunostaining for p-S6 and p-ERK, as indicated. (**H**) Prostate tissue weights, showing mean ± SEM, with *P* value indicated. (**I**) Percentage of proliferating cells as determined by Ki67 staining, showing mean ± SEM, with *P* value indicated. (**J**–**Q**) Studies done in a complementary tissue recombination model. (**J**) Diagram of the experimental strategy. (**K**–**P**) Representative tissue sections from the tissue recombinants made from the *Nkx3.1*$^{+/-}$*Pten*$^{+/-}$ prostate epithelium showing histological phenotype (H&E) and immunostaining for p-S6K and p-ERK, as indicated. (**Q**) Weights of the tissue graphs, showing mean ± SEM, with *P* value indicated. Scale bars: 100 μm.

Although conventional chemotherapeutic approaches have been proven effective in many contexts, now including prostate cancer (5, 6, 38), it has become increasingly evident that ultimately the most effective and safest long-term treatment options for cancer patients will be achieved by targeting the specific networks that are deregulated in tumors, as exemplified by the now classic example of Gleevec for the treatment of leukemia (39). However, targeted therapies using single agents often lead to resistance, as also exemplified by Gleevec (40). It has been proposed that tumor resistance can be circumvented, at least in part, using agents in combination that can simultaneously target multiple pathways — the idea being that coordinate suppression of multiple pathways may minimize the chances of developing resistant tumor cells.

This general strategy of combination therapy requires knowledge of relevant signaling networks that are deregulated in particular cancers, an understanding of how their coordinate and/or cooperative activities contribute to tumorigenesis, and relevant in vivo model systems to test the functional consequences of therapeutic targeting of such pathways for tumorigenesis. Indeed, while informative analyses in tumor cells in culture may provide mechanistic insights, studies done in the context of the tumor microenvironment in the whole

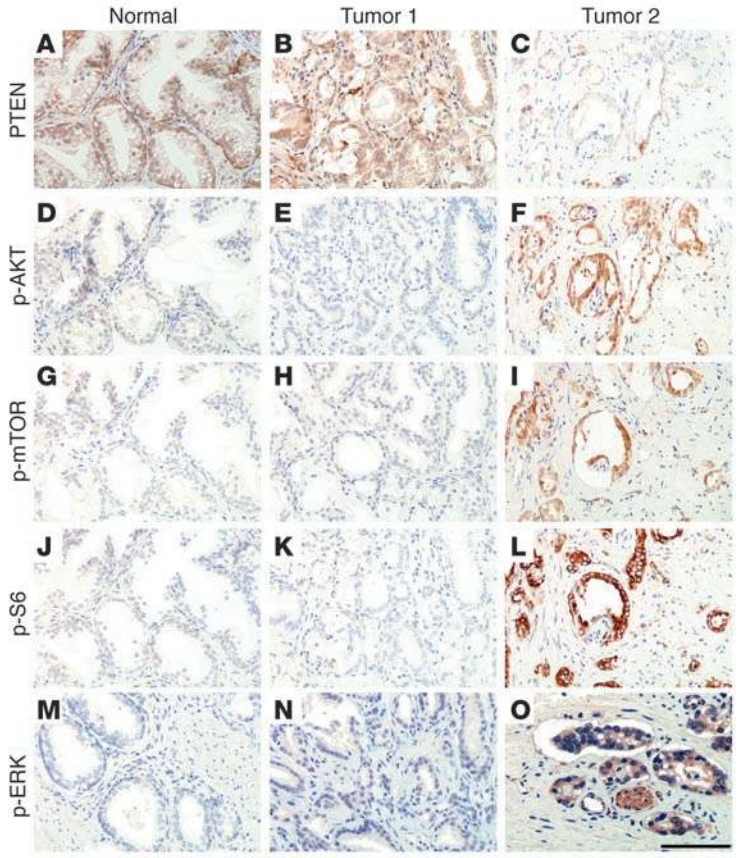

Figure 8
AKT/mTOR pathway activation is associated with human prostate cancer progression and correlated with activation of ERK MAPK. (**A**–**L**) Expression of PTEN and components on the AKT/mTOR signaling pathway in human normal and primary prostate cancer samples. Representative adjacent sections from the specimens used for the TMAs show staining for the indicated proteins. Shown are examples of benign prostatic tissue (Normal), a tumor without activation of the PTEN/AKT/mTOR pathway (Tumor 1), and a tumor with activation of this pathway (Tumor 2). Note that the expression of PTEN is inversely correlated with expression of p-AKT, p-mTOR, and p-S6. (**M**–**O**) Expression of p-ERK activation on semiadjacent sections of the same specimens. Note that, in these samples, p-ERK activation is well correlated with activation of components of the AKT/mTOR signaling pathway. Scale bar: 100 μm.

organism are likely to provide more robust strategies for predicting the efficacy of combinatorial inhibition for tumor growth in vivo. In this regard, analyses of relevant genetically engineered mutant mouse models may be informative for predicting both the pathways that may be effectively targeted and the therapeutic efficacy of single and combinatorial inhibition of such pathways (41–44).

Indeed, our current analyses exemplify the value of this general approach, as we have effectively used the *Nkx3.1; Pten* mutant mouse model both to define the functional significance of the AKT/mTOR and ERK MAPK signaling pathways for prostate tumorigenicity and to demonstrate the profound antitumorigenic consequences of combinatorial inhibition of these pathways for prostate tumorigenicity. Importantly, our findings show that the combination therapy is considerably more effective than the single agents with respect to their antitumorigenic activity, which appears to reflect in part their effects on the expression of the apoptotic regulator Bim. Further insights regarding the mechanisms underlying the striking synergism of these pathways is provided by the accompanying article by Carracedo and colleagues, who report that these pathways are modulated by a negative feedback loop (45).

More generally, an important consideration when using combination targeted therapy is that, more so than for conventional chemotherapy, the efficacy of the treatment for any single individual is likely to depend upon whether the specific pathways are deregulated in tumors from such individuals. Thus, accurate evaluation of the efficacy of targeted therapies is likely to depend on knowledge of the status of the relevant pathways prior to the onset of treatment, since clinical success or failure may well depend upon the status of such pathways. Indeed, our findings showing that activation of relevant target proteins in the AKT/mTOR and/or ERK MAPK signaling pathways can be readily detected in primary tumors from human prostate cancer patients (see Figure 8) demonstrate the feasibility of this approach and provides an effective screening tool for both enrolling patients in clinical trials and evaluating the outcome of such trials.

Table 2
Summary of TMA data

Pathology	No. of cases	PTEN (neg)	p-AKT (pos)	p-mTOR (pos)	p-S6 (pos)	p-ERK (pos)
BPH	25	0%	28%	20%	8%	40%
PIN	7	0%	43%	14%	14%	43%
Low-grade cancer	19	37%	63%	42%	32%	74%
High-grade cancer	19	22%	79%	53%	53%	68%

neg, negative; pos, positive.

Table 3
Correlation of staining on TMA

Correlation	p-AKT	p-mTOR	p-S6	p-ERK
p-AKT	ND	67%	67%	73%
p-mTOR	100%	ND	70%	60%
p-S6	100%	70%	ND	60%
p-ERK	85%	43%	57%	ND

ND, not determined.

Furthermore, our analyses of pathway activation in human prostate cancer have shown that a large percentage of advanced tumors display activation of AKT/mTOR and/or ERK MAPK signaling networks and predict that a large percentage of prostate cancer patients (>20%) will be appropriate candidates for treatment with agents that target these signaling pathways. Extrapolating from preclinical trials in the *Nkx3.1; Pten* mutant mice to the design of relevant clinical trials, we infer that combination therapy targeting AKT/mTOR and ERK MAPK signaling should be optimal for patients with hormone-refractory disease. Conceivably, combination therapy may be effective when used in conjunction with chemotherapy, as there are now several ongoing trials combining chemotherapy with mechanism-based approaches (4).

Notably, at present, the reason(s) for the enhanced efficacy of this combination therapy in prostate cancer in conditions of limiting androgens are unclear. Presumably, this reflects, at least in part, the fact that these pathways may be preferentially activated in hormone-refractory prostate cancer (8, 11, 13–15). However, it seems likely that there may be mechanistic bases that are dependent on the tissue context, such as potential variations in the activity levels of these kinases in the presence or absence of androgens (46). Regardless, our findings showing the efficacy of this combination treatment when provided simultaneously with androgen ablation (Figure 7) raise the exciting possibility that combination therapy targeting AKT/mTOR and MEK/ERK MAPK signaling may even be effective in an adjuvant therapy model for hormone-refractory disease.

In summary, our findings as well as recent work by Stommel and colleagues and Shah and colleagues (47, 48) highlight the value of pathway-targeted combination therapy to achieve maximal blockade of signaling pathways for cancer treatment. Furthermore, our study demonstrates the value of pursuing hypothesis-based preclinical trials in genetically engineered mutant mice that share relevant features with the human cancers that they represent.

Methods

Mouse models. All experiments using mice were approved by the Institutional Review Board of Columbia University Medical College. The *Nkx3.1; Pten* compound mutant mice have been described previously (15, 17, 18). Preclinical studies were done in a mixed strain background (C57BL/6 × 129S/V) using cohorts assembled from littermates of wild-type ($Nkx3.1^{+/+}Pten^{+/+}$) and mutant ($Nkx3.1^{-/-}Pten^{+/-}$ or $Nkx3.1^{+/-}Pten^{+/-}$) mice at 10–12 months of age that had been housed together and subjected to identical environmental conditions. Mice were randomly assigned to the androgen-intact group or the androgen-independent group; the latter were surgically castrated to remove the testes and epididymis, which is the source of endogenous androgens. Tissue recombinants were made using prostate epithelium from mutant or wild-type mice and rat embryonic mesenchyme and grown in androgen-intact or androgen-deprived (castrated) *nude* male hosts, as described previously (15, 17).

Preclinical trial design and analyses. Rapamycin was purchased from LC Laboratories (catalog R-5000, lots ASW-105 and ASW-109); PD0325901 was a generous gift from Pfizer (Batch U). Rapamycin was dissolved in 100% ethanol to make a working stock of 25 mg/ml and then diluted to 1.25 mg/ml in a solution of 5.2% Tween-80, 5.2% PEG400 in sterile water and delivered i.p. at 10 mg/kg. PD0325901 was dissolved in 0.05% hydroxy-propyl-methylcellulose, 0.02% Tween-80 in sterile water to make a working stock of 1.5 mg/ml and delivered via oral gavage at 20 mg/kg. Agents (or vehicle) were delivered for 5 consecutive days, with 2 days off for a period of 3 weeks. Mice were weighed daily and observed for signs of distress following dosing. Notably, none of the treatment paradigms resulted in appreciable weight loss (i.e., greater than 10%) in the mutant mice (Supplemental Table 1).

At the conclusion of the study, mice were sacrificed, prostate tissues were collected and photographed, and the wet weights of the prostate tissues were determined. For the tissue recombinant models, the graphs were removed from the kidney prior to weighing. The prostatic lobes (anterior, dorsolateral, and ventral) were collected individually and bilaterally; one lobe was fixed in formalin and paraffin-embedded for histology and immunohistochemistry and the other snap frozen in liquid nitrogen for Western blotting. All analyses were done using both the anterior and dorsolateral prostatic lobes; histological and immunohistochemical analyses are shown for the anterior prostate and Western blot analyses for the dorsolateral gland.

Immunohistochemical studies, Western blot analyses, and semiquantitative analyses of the histological phenotype were done as described previously (15, 17, 18). Briefly, for grading of the histological phenotype, a minimum of 4 random sections from different locations in the prostate tissues were examined for each experimental animal. The phenotype was scored based on analyses of the multiple sections in each animal plus the analyses of all animals, following which a representative tissue section was selected to illustrate the phenotype. Analyses of the immunohistochemical studies were done using 2–3 independent sections from each of 4 experimental animals in each group. For quantification of proliferating cells, slides were immunostained with Ki67, and cells were counted as described previously (49) in a minimum of 10 independent sections from 5 independent mice (i.e., 50 sections), with results expressed as the percentage of Ki67-labeled epithelium relative to total epithelium, visualized using hematoxylin.

Antibodies used in this study were: p-p44/42 MAPK (Thr202/Tyr204) antibody (catalog 9101 or IHC preferred antibody 4376; 1:200), p44/42 MAPK antibody (catalog 9102), p-AKT (Ser473) antibody (catalog 9271 or IHC preferred antibody 3787; 1:50), and p-S6 Ribosomal Protein (Ser235/236) antibody (catalog 2211; 1:250), all from Cell Signaling Technology; Bim antibody (catalog 2065; 1:500) from ProSci Inc.; and NCL-Ki67p (1:1,500) from Novocastra (Leica Microsystems).

Cell culture analyses. Cytotoxicity assays were performed using the CASP 2.1 or 1.1 line (15, 19). Exponentially growing cells were seeded into 96-well plates at 800 cells/well in 100 μl growth medium in the presence or absence of dihydrotestosterone. Rapamycin or PD0325901 was serially diluted in media, and the cells were maintained at 37°C for 96 hours. Cell density was determined following addition of 20 μl MTS reagent (Promega) by measurement of the absorbance at 490-nm wavelength. The IC_{50} was deter-

Table 4
Activation of pathways in patient specimens

Activated	Cases (%)
Neither the PTEN pathway nor ERK[A]	8
PTEN pathway and ERK[B]	21
PTEN pathway (partial) and ERK	42

[A]e.g., tumor 1 in Figure 8. [B]e.g., tumor 2 in Figure 8.

mined using the software SoftMax (Molecular Devices). For combination drug treatment, rapamycin plus PD0325901 was diluted in the growth medium at a fixed ratio of doses (IC_{50} versus IC_{50}). The CI was calculated based on the Chou-Talalay equation (34) using CalcuSyn software (Biosoft). For Bim-knockdown studies, CASP 1.1 and 2.1 cells were transfected with 50 nM of control or Bim siRNA (Santa Cruz Biotechnology Inc.), according to the manufacturer's protocol. One day after transfection, cells were treated with rapamycin and/or PD0325901 for 48 hours. Cytotoxity assays were performed using a Cell Growth Determination Kit, MTT Based (Sigma-Aldrich), according to the manufacturer's protocol.

Human TMAs. The human TMAs were made using samples from prostatectomy specimens obtained from the Molecular Pathology Tumor Bank of Columbia University. All studies of human tissue were approved by the Institutional Review Board of Columbia University Medical Center. To construct the TMAs, sections of normal prostate and tumor tissue that were embedded in paraffin and stained with H&E were reviewed to identify viable, morphologically representative areas of the specimen from which needle core samples could be taken. From each specimen, triplicate tissue cores with diameters of 0.6 mm were punched and arrayed onto a recipient paraffin block using a precision instrument (Beecher Instruments). Five-micrometer sections of these TMA blocks were stained with H&E or used for immunohistochemical analysis. Prostate tumor samples included PIN and PCa, which was classified as having either a low Gleason (≤6) or high Gleason (>7) score.

Two TMAs were used for the present study. The first included 70 prostate samples: 25 BPH cases, 7 PIN lesions, and 38 PCas (19 displayed a low Gleason score and 19 a high Gleason score). Each tissue was represented by 3 independent cores in each TMA. The second TMA included 535 prostate samples: 65 corresponded to BPH, 78 to PIN, and 392 to PCas (181 cases corresponded to organ-confined prostate cancer, 120 cases to hormone-refractory prostate cancer, and 91 cases to metastatic prostate cancer). Seven consecutive sections of the 2 TMAs were cut and stained with H&E (verification of histopathology), used as a negative control, or stained with immunohistochemical markers.

Immunohistochemical analyses were performed following the standard avidin-biotin immunoperoxidase staining procedure. Briefly, TMA slides were deparaffinized and then submitted to antigen retrieval by steamer treatment for 15 minutes in 10 mM citrate buffer at pH 6.0, followed by primary antibody incubation overnight at 4°C. Then slides were incubated with biotinylated anti-rabbit or anti-mouse immunoglobulins at a 1:1,000 dilution for 30 minutes (Vector Laboratories Inc.) followed by avidin-biotin peroxidase complexes at a 1:25 dilution (Vector Laboratories Inc.) for 30 minutes. Diaminobenzidine was used as the chromogen and hematoxylin as a nuclear counterstain. Primary antibodies used were against PTEN (Ab-6, mouse clone 6H2.1; Neomarkers, Thermo Scientific; 1:50), p-AKT (Ser473, rabbit polyclonal; Cell Signaling Technology; 1:50), p-mTOR (Ser 2448, rabbit clone 49F9; Cell Signaling Technology; 1:50), S6K (rabbit polyclonal; Cell Signaling Technology; 1:75), and p44/42 MAPK (rabbit clone 137F5; Cell Signaling Technology; 1:100).

The immunoreactivity for each antibody was scored according to the percentage of cells displaying a positive immunostaining profile (from undetectable [0%] to homogeneous expression [100%]) and the intensity of the staining (0, 1+, 2+, and 3+). Average values of the 3 representative cores from each arrayed sample were used for statistical analyses. Expression values were displayed as mean values accompanied by 95% confidence intervals and range. The relationship between immunohistochemical results and clinical parameters was analyzed using the nonparametric Wilcoxon–Mann-Whitney *U* tests. A *P* value of less than 0.05 was considered statistically significant.

Acknowledgments

We are indebted to Pfizer for sharing the PD325901 compound. We thank Mitchell Benson, Edward Gelmann, Daniel Petrylak, and Michel Shen for comments on the manuscript. This work was supported in part by National Cancer Institute (NCI) grants to C. Abate-Shen (U01-CA84294 and R01-CA115717), as well as funding from the T.J. Martell Foundation. C. Cordon-Cardo and his laboratory are, in part, supported by the NCI SPORE CA92629 grant in Prostate Cancer and grants from The T.J. Martell Foundation and the Sands Family Foundation. A. Puzio-Kuter was supported by 1F31CA110625-01 Ruth L. Kirschstein National Research Service Award. T.H. Foster was supported, in part, by the Swiss National Science Foundation (81BS-69441) and the Swiss Urologic Association.

Received for publication December 14, 2007, and accepted in revised form June 25, 2008.

Address correspondence to: Cory Abate-Shen, Columbia University College of Physicians and Surgeons, Herbert Irving Comprehensive Cancer Center, 1130 St. Nicholas Avenue, Room 217A, New York, New York 10032, USA. Phone: (212) 851-4731; Fax: (212) 851-4572; E-mail: cabateshen@columbia.edu.

1. DeMarzo, A.M., Nelson, W.G., Isaacs, W.B., and Epstein, J.I. 2003. Pathological and molecular aspects of prostate cancer. *Lancet.* **361**:955–964.
2. Gelmann, E.P. 2002. Molecular biology of the androgen receptor. *J. Clin. Oncol.* **20**:3001–3015.
3. Scher, H.I., and Sawyers, C.L. 2005. Biology of progressive, castration-resistant prostate cancer: directed therapies targeting the androgen-receptor signaling axis. *J. Clin. Oncol.* **23**:8253–8261.
4. Petrylak, D.P. 2007. New paradigms for advanced prostate cancer. *Rev. Urol.* **9**(Suppl. 2):S3–S12.
5. Pienta, K.J., and Smith, D.C. 2005. Advances in prostate cancer chemotherapy: a new era begins. *CA Cancer J. Clin.* **55**:300–318; quiz 323–305.
6. Berry, W.R. 2005. The evolving role of chemotherapy in androgen-independent (hormone-refractory) prostate cancer. *Urology.* **65**(6 Suppl.):2–7.
7. Petrylak, D.P. 2005. The current role of chemotherapy in metastatic hormone–refractory prostate cancer. *Urology.* **65**(5 Suppl.):3–7; discussion 7–8.
8. Malik, S.N., et al. 2002. Immunohistochemical demonstration of phospho-Akt in high Gleason grade prostate cancer. *Clin. Cancer Res.* **8**:1168–1171.
9. McMenamin, M.E., et al. 1999. Loss of PTEN expression in paraffin-embedded primary prostate cancer correlates with high Gleason score and advanced stage. *Cancer Res.* **59**:4291–4296.
10. Kremer, C.L., et al. 2006. Expression of mTOR signaling pathway markers in prostate cancer progression. *Prostate.* **66**:1203–1212.
11. Paweletz, C.P., et al. 2001. Reverse phase protein microarrays which capture disease progression show activation of pro-survival pathways at the cancer invasion front. *Oncogene.* **20**:1981–1989.
12. Gioeli, D. 2005. Signal transduction in prostate cancer progression. *Clin. Sci. (Lond.).* **108**:293–308.
13. Gioeli, D., Mandell, J.W., Petroni, G.R., Frierson, H.F., Jr., and Weber, M.J. 1999. Activation of mitogen-activated protein kinase associated with prostate cancer progression. *Cancer Res.* **59**:279–284.
14. Abreu-Martin, M.T., Chari, A., Palladino, A.A., Craft, N.A., and Sawyers, C.L. 1999. Mitogen-activated protein kinase kinase kinase 1 activates androgen receptor-dependent transcription and apoptosis in prostate cancer. *Mol. Cell. Biol.* **19**:5143–5154.
15. Gao, H., et al. 2006. Combinatorial activities of Akt and B-Raf/Erk signaling in a mouse model of androgen-independent prostate cancer. *Proc. Natl. Acad. Sci. U. S. A.* **103**:14477–14482.
16. Uzgare, A.R., and Isaacs, J.T. 2004. Enhanced redundancy in Akt and mitogen-activated protein kinase-induced survival of malignant versus normal prostate epithelial cells. *Cancer Res.* **64**:6190–6199.
17. Abate-Shen, C., et al. 2003. Nkx3.1; Pten mutant mice develop invasive prostate adenocarcinoma and lymph node metastases. *Cancer Res.* **63**:3886–3890.
18. Kim, M.J., et al. 2002. Cooperativity of Nkx3.1 and Pten loss of function in a mouse model of prostate carcinogenesis. *Proc. Natl. Acad. Sci. U. S. A.* **99**:2884–2889.
19. Gao, H., et al. 2004. A critical role for p27kip1 gene dosage in a mouse model of prostate carcinogenesis. *Proc. Natl. Acad. Sci. U. S. A.* **101**:17204–17209.
20. Kuzmichev, A., et al. 2005. Composition and histone substrates of polycomb repressive group complexes change during cellular differentiation. *Proc. Natl. Acad. Sci. U. S. A.* **102**:1859–1864.
21. Ouyang, X., et al. 2008. Activator protein-1 transcription factors are associated with progression and recurrence of prostate cancer. *Cancer Res.* **68**:2132–2144.
22. Sebolt-Leopold, J.S., and Herrera, R. 2004. Targeting the mitogen-activated protein kinase cascade to treat cancer. *Nat Rev Cancer* **4**:937–947.
23. Kohno, M., and Pouyssegur, J. 2006. Targeting the

ERK signaling pathway in cancer therapy. *Ann Med.* **38**:200–211.
24. Solit, D.B., et al. 2006. BRAF mutation predicts sensitivity to MEK inhibition. *Nature.* **439**:358–362.
25. Hay, N., and Sonenberg, N. 2004. Upstream and downstream of mTOR. *Genes Dev.* **18**:1926–1945.
26. Skeen, J.E., et al. 2006. Akt deficiency impairs normal cell proliferation and suppresses oncogenesis in a p53-independent and mTORC1-dependent manner. *Cancer Cell.* **10**:269–280.
27. Sawyers, C.L. 2003. Will mTOR inhibitors make it as cancer drugs? *Cancer Cell.* **4**:343–348.
28. Fan, Q.W., et al. 2007. A dual phosphoinositide-3-kinase alpha/mTOR inhibitor cooperates with blockade of epidermal growth factor receptor in PTEN-mutant glioma. *Cancer Res.* **67**:7960–7965.
29. Neshat, M.S., et al. 2001. Enhanced sensitivity of PTEN-deficient tumors to inhibition of FRAP/mTOR. *Proc. Natl. Acad. Sci. U. S. A.* **98**:10314–10319.
30. Podsypanina, K., et al. 2001. An inhibitor of mTOR reduces neoplasia and normalizes p70/S6 kinase activity in Pten$^{+/-}$ mice. *Proc. Natl. Acad. Sci. U. S. A.* **98**:10320–10325.
31. Kwon, C.H., Zhu, X., Zhang, J., and Baker, S.J. 2003. mTor is required for hypertrophy of Pten-deficient neuronal soma in vivo. *Proc. Natl. Acad. Sci. U. S. A.* **100**:12923–12928.
32. Majumder, P.K., et al. 2004. mTOR inhibition reverses Akt-dependent prostate intraepithelial neoplasia through regulation of apoptotic and HIF-1-dependent pathways. *Nat. Med.* **10**:594–601.
33. Brown, A.P., Carlson, T.C., Loi, C.M., and Graziano, M.J. 2007. Pharmacodynamic and toxicokinetic evaluation of the novel MEK inhibitor, PD0325901, in the rat following oral and intravenous administration. *Cancer Chemother. Pharmacol.* **59**:671–679.
34. Chou, T.C., and Talalay, P. 1984. Quantitative analysis of dose-effect relationships: the combined effects of multiple drugs or enzyme inhibitors. *Adv. Enzyme Regul.* **22**:27–55.
35. Gelinas, C., and White, E. 2005. BH3-only proteins in control: specificity regulates MCL-1 and BAK-mediated apoptosis. *Genes Dev.* **19**:1263–1268.
36. White, E. 2006. Mechanisms of apoptosis regulation by viral oncogenes in infection and tumorigenesis. *Cell Death Differ.* **13**:1371–1377.
37. Tan, T.T., et al. 2005. Key roles of BIM-driven apoptosis in epithelial tumors and rational chemotherapy. *Cancer Cell.* **7**:227–238.
38. Petrylak, D.P. 2005. Chemotherapy for androgen-independent prostate cancer. *World J. Urol.* **23**:10–13.
39. Druker, B.J., et al. 2001. Activity of a specific inhibitor of the BCR-ABL tyrosine kinase in the blast crisis of chronic myeloid leukemia and acute lymphoblastic leukemia with the Philadelphia chromosome. *N. Engl. J. Med.* **344**:1038–1042.
40. Gorre, M.E., et al. 2001. Clinical resistance to STI-571 cancer therapy caused by BCR-ABL gene mutation or amplification. *Science.* **293**:876–880.
41. Abate-Shen, C. 2006. A new generation of mouse models of cancer for translational research. *Clin. Cancer Res.* **12**:5274–5276.
42. Carver, B.S., and Pandolfi, P.P. 2006. Mouse modeling in oncologic preclinical and translational research. *Clin. Cancer Res.* **12**:5305–5311.
43. Fomchenko, E.I., and Holland, E.C. 2006. Mouse models of brain tumors and their applications in preclinical trials. *Clin. Cancer Res.* **12**:5288–5297.
44. Olive, K.P., and Tuveson, D.A. 2006. The use of targeted mouse models for preclinical testing of novel cancer therapeutics. *Clin. Cancer Res.* **12**:5277–5287.
45. Carracedo, A., et al. 2008. Inhibition of mTORC1 leads to MAPK pathway activation through a PI3K-dependent feedback loop in human cancer. *J. Clin. Invest.* **118**:3065–3074.
46. Xu, Y., Chen, S.Y., Ross, K.N., and Balk, S.P. 2006. Androgens induce prostate cancer cell proliferation through mammalian target of rapamycin activation and post-transcriptional increases in cyclin D proteins. *Cancer Res.* **66**:7783–7792.
47. Stommel, J.M., et al. 2007. Coactivation of receptor tyrosine kinases affects the response of tumor cells to targeted therapies. *Science.* **318**:287–290.
48. Shah, N.P., et al. 2007. Sequential ABL kinase inhibitor therapy selects for compound drug-resistant BCR-ABL mutations with altered oncogenic potency. *J. Clin. Invest.* **117**:2562–2569.
49. Bhatia-Gaur, R., et al. 1999. Roles for Nkx3.1 in prostate development and cancer. *Genes Dev.* **13**:966–977.